nature climate change

Article

https://doi.org/10.1038/s41558-024-02193-x

Different technology packages for aluminium smelters worldwide to deliver the 1.5 °C target

Received: 12 March 2024

Accepted: 23 October 2024

Published online: 2 January 2025

Check for updates

Chang Tan[1], Xiang Yu[2,3] ✉, Dan Li[4], Tianyang Lei[5], Qi Hao[1] & Dabo Guan[1,5] ✉

Production of aluminium, one of the most energy-intensive metals, is challenging for mitigation efforts. Regional mitigation strategies often neglect the emissions patterns of individual smelters and fail to guide aluminium producers' efforts to reduce GHG emissions. Here we build a global aluminium GHG emissions inventory (CEADs-AGE), which includes 249 aluminium smelters, representing 98% of global primary aluminium production and 280 associated fossil fuel-based captive power units. We find, despite the installation of more efficient and higher amperage cells, that the share of aluminium production powered by fossil fuel-based captive power units increased from 37% to 49% between 2012 and 2021. Retiring fossil fuel-based captive power plants 10 years ahead of schedule could reduce emissions intensity by 5.0–10.5 tCO_2e per tonne of aluminium for dependent smelters. At least 18% of smelting capacity by 2040 and 67% by 2050 must be retrofitted with inert anode technology to achieve net-zero targets.

Aluminium, the second most-used metal after steel, is integral to various industries[1,2], including clean energy infrastructures[3–6] such as photovoltaic panels[7–9] and electric vehicles[10,11], which are driving increased aluminium demand[12]. Owing to its high chemical reactivity, the energy required to produce aluminium can be up to ten times greater per tonne than that for crude steel[13–15]. The primary method for aluminium production is the Hall–Héroult process[16,17], involving the dissolution of aluminium oxide in molten salts at ~960 °C and the application of electrical current to facilitate the reaction[18].

Recent advancements have focused on optimizing cell designs[19–21], electrode configurations[22–26] and operational adaptability[27–29] to reduce the energy intensity of the Hall–Héroult process[30]. However, the benefits of reduced energy intensity are offset by the increased use of fossil fuel-based captive power plants, which have reduced the share of non-fossil energy in the aluminium industry from 60% to 33% over the past three decades[14]. Additionally, the electrolysis process emits not only CO_2 but also perfluorocarbons (PFCs), which have a substantially higher global warming potential than CO_2 (refs. 31,32).

Given the growing demand for aluminium, technological innovations in production are important. Mitigation efforts at the facility level are crucial because of their direct impact on the production processes adopted. We developed a smelter-based bottom-up global aluminium GHG emissions inventory (CEADs-AGE), which includes 249 aluminium smelters and 280 associated fossil fuel-based captive power units. This inventory covers a wide range of technologies and configurations, providing a detailed assessment of emissions at the facility level. Our study utilizes the latest smelter survey data to compile GHG emissions inventory, identifying patterns and presenting tailored mitigation strategies for global aluminum smelters. Detailed methodology and data descriptions are provided in the Methods section.

[1]Department of Earth System Science, Ministry of Education Key Laboratory for Earth System Modeling, Institute for Global Change Studies, Tsinghua University, Beijing, China. [2]University of Chinese Academy of Social Sciences, Beijing, China. [3]Research Institute for Eco-civilization (RIEco), Chinese Academy of Social Sciences, Beijing, China. [4]China Nonferrous Metals Industry Association, Beijing, China. [5]The Bartlett School of Sustainable Construction, University College London, London, UK. ✉e-mail: yuxiang@cass.org.cn; guandabo@tsinghua.edu.cn

https://doi.org/10.1038/s41558-024-02193-x

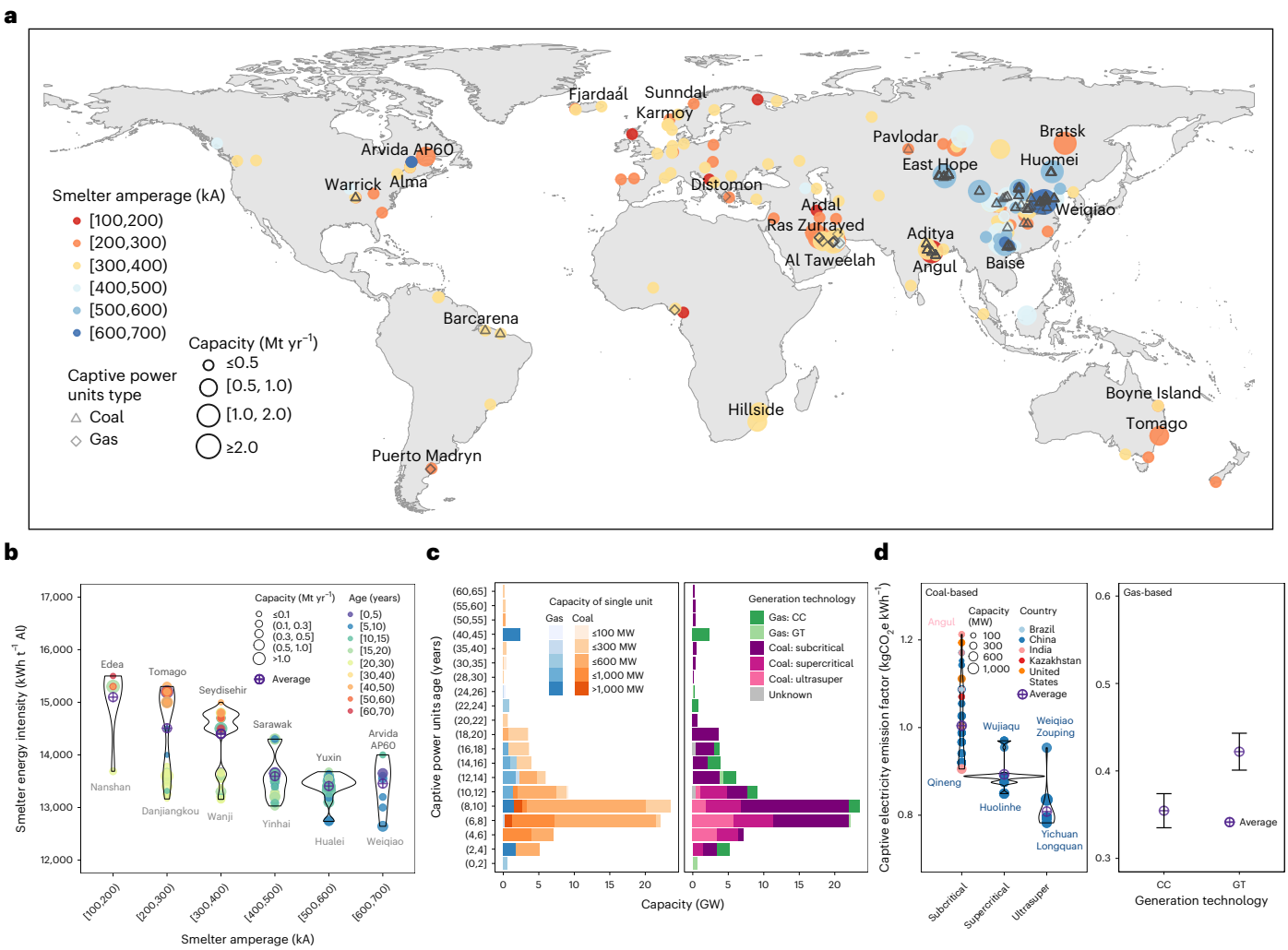

Fig. 1 | Technology and emission patterns of global aluminium smelters and their fossil fuel-based captive power units in 2021. a, Geographical distribution of aluminium smelters and fossil fuel-based captive power units. Icons may overlap because of the close proximity of many units. **b**, Energy intensity of smelters categorized by different age groups within each amperage category. **c**, Distribution of captive power units by installed capacity (left) and generation technology type (right), across different age groups. **d**, Electricity generation emission factors for coal-based (left, by unit) and gas-based (right, with the error bars showing maximum and minimum emissions intensity range from literatures) captive power units, categorized by generation technology. The average energy intensity of each smelter amperage group and the average electricity emission factor of each generation technology are shown by purple dots in **b** and **d**, respectively.

Technologies and emission patterns

In 2021, global primary aluminium smelting capacity reached 81 Mt yr^{-1} and with total emissions of 651 $MtCO_2e$, comprising 82% electricity-related emissions and 18% process-related emissions (Supplementary Fig. 1). Global aluminium smelters are increasingly adopting higher amperage, with smelters using currents >400 kA now accounting for 64% of smelting capacity in facilities <20 years old (Fig. 1b). The adoption of higher amperage technology is aimed at improving current efficiency and reducing energy intensity. Smelters with currents of [200, 300), [300, 400), [400, 500) and [500, 600) kA exhibit 4%, 5%, 10% and 11% lower energy intensity, respectively, compared to those <200 kA (purple dots in Fig. 1b). The 600+ kA cell, a breakthrough technology in the last decade, can reduce substantially smelting energy intensity to 12,630 kWh per tonne of aluminium, as demonstrated by the Weiqiao (Shandong) smelter in China, one of the most energy-efficient smelters today (Fig. 1b). Currently, 90% of the smelting capacity using amperages >400 kA is in China, making it the most energy-efficient country in terms of aluminium production (Fig. 1a).

In 2021, we identified 91 GW of operational captive thermal power capacity (Fig. 1c), supporting 49% global aluminium production. This share has increased by 12% over the past decade, up from 37% in 2012. Of this capacity, 70 GW was built after 2010, meaning that these units are still relatively young. The majority (85%) of total captive power capacity is coal-based, primarily subcritical units, which accounts for 51% of the total captive power capacity (Fig. 1c). Supercritical and ultrasupercritical units, which operate at higher pressures and temperatures for increased thermal efficiency[33], make up 21% and 13% of captive generation capacity, respectively, and have 13–25% lower emission factors than subcritical technologies (Fig. 1d). Supercritical and ultrasupercritical units have seen increased adoption in China, particularly in the (6, 12] years age group. In India, 85% of aluminium capacity is supported by coal-based subcritical captive power units, combined with [300, 400) kA cell configurations, placing India at the top of the ranking for aluminium smelting emissions intensity (Extended Data Fig. 1). Gas-based captive power units constitute 15% of the total capacity, with 92% located in the Middle East. Notably, 90% of gas-fired power units use combined cycle gas turbine (CC) technology, which offers 12–15% higher efficiency than standard gas turbine (GT) technology by using waste heat for additional electricity generation (Fig. 1d).

https://doi.org/10.1038/s41558-024-02193-x

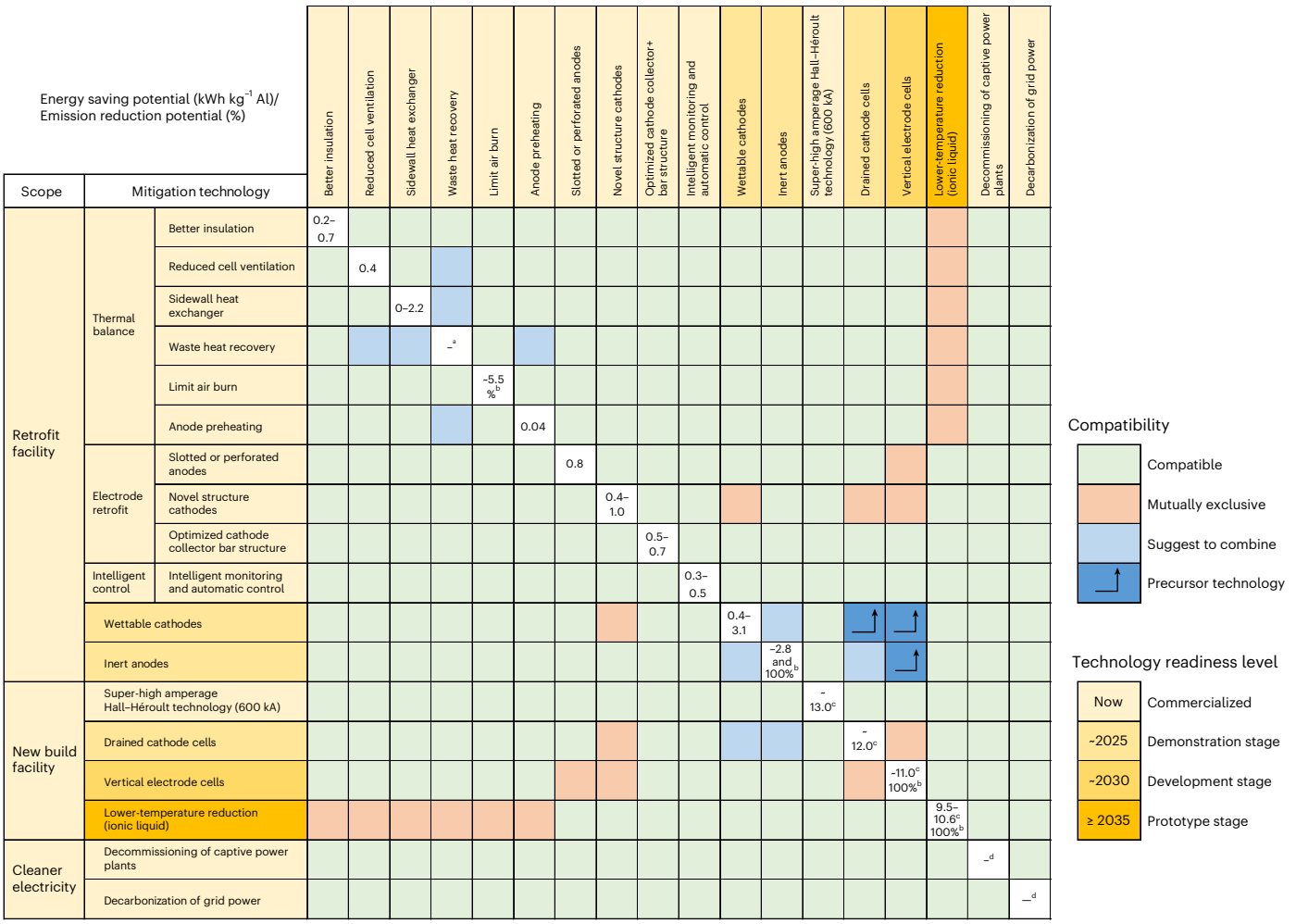

Fig. 2 | Key mitigation technologies for aluminium smelters. The shades of yellow represent the technology readiness level. The horizontal and vertical axes list the same set of technologies. Compatibility among technologies is indicated by colour: light green denotes compatibility, light pink denotes incompatibility, light blue indicates that the technologies can be used independently but are recommended to be combined for greater emissions reduction and dark blue indicates that the technology on the vertical axis is a prerequisite for the one on the horizontal axis. The numbers in the white areas represent the energy-saving potential of a retrofit technology, the energy intensity of new cell designs (in kWh kg^{-1} Al) or the emissions reduction potential (in %) of a specific technology. [a]Depend on the source of waste heat. [b]Process-related emission reduction. [c]Reduce cell smelting energy intensity to this value. [d]Depend on the specific situation of captive power plants and local power grid.

Smelters in different regions, each operating with distinct cell designs and energy sources, face unique mitigation challenges, underscoring the need for tailored mitigation strategies for each facility.

Mitigation technology packages

The future GHG emissions of a smelter are influenced by the adopted mitigation technology, electricity source and the output level of the smelter[34–36] (Extended Data Fig. 2).

Choice of mitigation technology for a smelter depends on the readiness level of the technology, the current cell configuration and the local climate mitigation ambitions. For example, the Alma smelter in Canada could be retrofitted with inert anode technology by 2030, leveraging the 450 kA industrial application programme led by its parent company, Rio Tinto[37], and Canada's goal of achieving carbon neutrality by 2050. In contrast, the Lanzhou aluminium smelter in China may not begin inert anode retrofitting until after 2040, as there is currently no evidence that its parent company, Chinalco, has mastered inert anode technology at an industrial level, and China's carbon neutrality target is set for 2060 (subscenario E_2; Methods).

The electricity source of a smelter is determined by its fossil fuel-based captive power plants and the regional electricity grid. Smelters typically prioritize self-generated electricity when available. For instance, the Aditya smelter in India may continue relying on its 6 × 150 MW coal-based supercritical power units, which began operation in 2014, until their decommissioning in 2044, assuming a 30 year lifespan[38,39] (default subscenario for captive power plant lifetime, L_{30}; Methods). After decommissioning, the Aditya smelter will transition to purchasing electricity from the regional power grid (Extended Data Fig. 3).

The production output of a smelter is influenced by its current capacity and the regional total output. Regional production is allocated to smelters on the basis of their energy efficiency, with the most efficient smelters prioritized until the demand for regional production is met. If existing capacity cannot satisfy the demand, new capacity will be constructed (Extended Data Fig. 3; Methods).

We compiled a key mitigation technology inventory for each of the 249 aluminium smelters, providing essential groundwork for differentiated mitigation packages (Fig. 2). This inventory aligns the compatibility of these technologies with the infrastructure of existing smelters. It includes essential retrofit technologies to optimize thermal balance, renew electrode configurations and enhance operational adaptability within current smelters. The inventory also introduces

Table 1 | Technology narrative pathway definition

Path no.	Path definition	Socioeconomic driver (SSP)	Captive power plant lifetime (L)	Existing smelter		New smelter
				Commercialized technologies (C)	Inert anode and wettable cathode (E)	Innovative cell design (I)
P1	Business as usual	SSP245	30 years (L_{30})	× (C_1)	× (E_1)	× (I_1)
P2	P1+SSP119	SSP119	30 years (L_{30})	× (C_1)	× (E_1)	× (I_1)
P3	P2+captive early retirement	SSP119	20 years (L_{20})	× (C_1)	× (E_1)	× (I_1)
P4	P3+energy efficiency improvement	SSP119	20 years (L_{20})	✓ (C_2)	× (E_1)	✓ (I_2)
P5	P4+process mitigation	SSP119	20 years (L_{20})	✓ (C_2)	✓ (E_2)	✓ (I_2)

four cutting-edge cell designs for new smelting capacities and two electricity decarbonization strategies for all smelters. Each technology is documented in detail, with key features such as energy or emissions reduction potential, technology readiness level and technology suitability and compatibility (Supplementary Section 3).

We analyse how various strategies, and their combinations, could influence the emissions trajectory by treating each scenario as a combination of subscenarios (Methods). We considered five socioeconomic subscenarios by combining different shared socioeconomic pathways (SSPs) and representative concentration pathways (RCPs), including SSP360 (SSP 3–RCP 6.0), SSP260 (SSP 2–RCP 6.0), SSP245 (SSP 2–RCP 4.5), SSP126 (SSP 1–RCP 2.6) and SSP119 (SSP 1–RCP 1.9). Each pathway represents a distinct developmental trajectory characterized by higher gross domestic product (GDP), lower population growth rates and increasing shares of renewable energy. These factors affect aluminium production projections and electricity generation, thereby influencing the GHG emissions trajectory.

In addition, we introduce four sets of technology application subscenarios, which include three subscenarios considering different lifetimes of captive power plants (L); two commercialized technology subscenarios (C); two inert anode and wettable cathode technology subscenarios (E); and two innovative cells design subscenarios (I). This framework results in a comprehensive analysis encompassing $5 \times 3 \times 2 \times 2 \times 2 = 120$ possible scenarios (Extended Data Fig. 2, orange part). From these, five technology narrative pathways are selected P1–P5 (Table 1). They are progressively related, with each one modifying part of the subscenarios, illustrating the emissions reduction potential of different mitigation strategies by cross-comparing them. Among them, P1 represents a business-as-usual (BAU) scenario without any additional mitigation strategies, while P5 represents the most aggressive mitigation scenario, in which the aluminium sector adopts all available strategies (see Methods for description of selected technology narrative pathways).

Emissions intensity decline of existing smelters

The emissions reduction potentials of various technology categories in four typical aluminium smelters under technology narrative pathways P1 and P5 are illustrated in Fig. 3 (Extended Data Fig. 4 provides details for P2, P3 and P4). Commercially available energy-saving technologies can achieve a 15–25% efficiency improvement for smelters, depending on their current cell configurations. However, the emissions reduction potential varies substantially among smelters, as it is closely tied to the source of electricity used. For smelters that predominantly rely on renewable energy sources, the reduction potential is limited. For example, the Alma smelter in Quebec, Canada, which already uses decarbonized electricity (with an electricity emission factor of ~0.001 $kgCO_2e\ kWh^{-1}$), shows no emissions reduction potential from energy-saving technologies (Fig. 3a, right). In contrast, energy-saving measures are crucial for smelters that depend on fossil fuel-based self-generated electricity, particularly in the short term. For instance, the Aditya smelter in India could achieve a reduction of 2.1 $tCO_2e\ t^{-1}$ Al by 2040 through the retrofitting of energy-saving technologies (Fig. 3d, right).

Long-lifetime fossil fuel-based captive power plants can lock in high emissions intensity for smelters over the next 10–20 years, preventing them from benefiting from the gradual decarbonization of regional electricity grids. As shown in Fig. 3, smelters such as Lanzhou Aluminium in China and Aditya in India, which currently operate with coal-based captive power plants, experience substantial emissions intensity reductions only when their captive power plants are decommissioned and they transition to grid electricity. This shift could deliver a reduction of 5.0–10.5 $tCO_2e\ t^{-1}$ Al for smelters supported by fossil fuel-based captive power plants by reducing electricity emission factors by 50–100% (Fig. 3c,d). Conversely, smelters such as Aldel in the Netherlands, which do not rely on fossil fuel-based captive power plants, could see decreasing emissions intensity from 2020 to 2050 without additional mitigation efforts due to the increasing penetration of renewable energy in the regional grid (Fig. 3b, left).

Achieving carbon-free aluminium production requires the retrofitting of smelters with inert anode technology, which could reduce emissions intensity by 1.3–1.8 $tCO_2e\ t^{-1}$ Al. The Alma smelter in Canada may be the first to benefit from such retrofitting, thanks to the inert anode demonstration projects by Alcoa and Rio Tinto (Fig. 3a, right). However, in regions where technology innovation is limited and the pursuit of carbon neutrality is delayed, smelters may postpone adopting technologies that are still in the demonstration or development stage. For example, by 2050, despite the decommissioning of six coal-based captive power units after a 20 year lifespan, the Aditya smelter in India may still face 1.8 $tCO_2e\ t^{-1}$ Al unmitigated process-related emissions under pathway P5 (Fig. 3d, right).

Global primary aluminium industry emissions pathways

If the global aluminium industry maintains its current technology levels, without adopting additional mitigation technologies and with the regional electricity structure and production level following the SSP245 scenario, total emissions could reach 675 Mt yr^{-1} by 2050, with 22.4 Gt of cumulative emissions from 2020 to 2050 (P1, Fig. 4). Although cumulative emissions during this period could decrease to 15.2 Gt if the regional electricity structure follows the SSP119 scenario (P2), this would still result in total emissions of 203 Mt yr^{-1} and a global average emissions intensity of 2.0 $tCO_2e\ t^{-1}$ Al by 2050. This scenario would lead to slow mitigation progress before 2045, as many existing captive power plants continue operating without abatement (P2, Fig. 4).

Retiring fossil fuel-based captive power plants a decade earlier than planned could result in an additional cumulative emissions reduction of up to 3.4 Gt (P2 versus P3, Fig. 4a), accounting for 28% of the total cumulative emissions reduction from P1 to P5. Reducing the lifespan of captive power plants from 30 to 20 years would require 26% of currently operating captive power units to cease operations by 2030 and 53% to be shut down between 2030 and 2035. This strategy would lead

https://doi.org/10.1038/s41558-024-02193-x

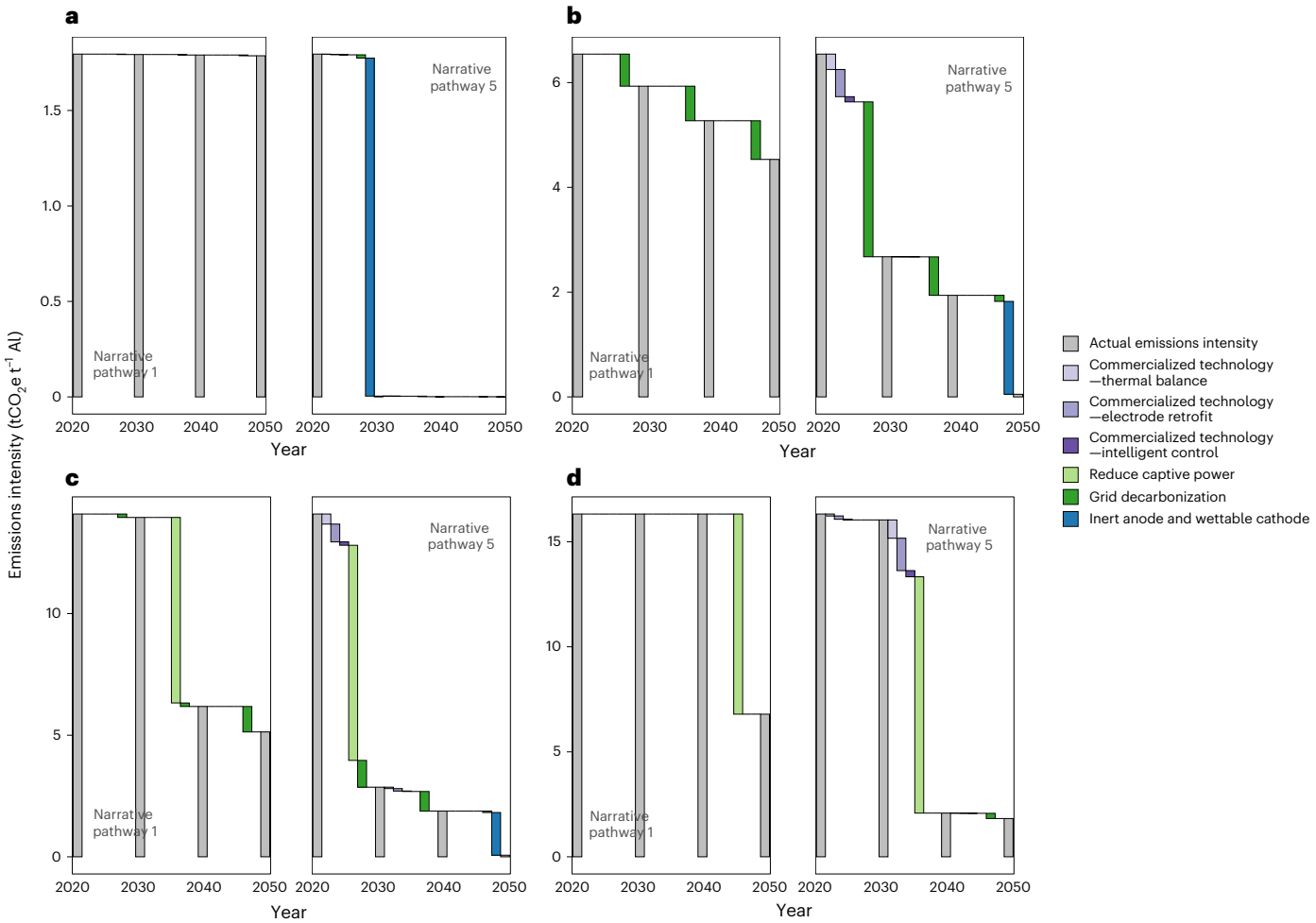

Fig. 3 | Technology emissions reduction contributions of four typical smelters. a–d, The contribution of different technologies to reducing the emissions intensity of smelter Alma, Canada (**a**); Aldel, the Netherlands (**b**); Lanzhou Aluminium, China (**c**); and Aditya, India (**d**), under narrative pathways P1 (SSP245, L_{30}, C_1, E_1, I_1) (left) and P5 (SSP119, L_{20}, C_2, E_2, I_2) (right).

to cumulative emissions reductions of 2.9 Gt for China and 0.3 Gt for India during 2020–2050 (P2 versus P3, Fig. 4d,e).

While power decarbonization through abated fossil fuel-based captive power plants and green grid is necessary, it is not sufficient to achieve carbon-free aluminium production. Additional cumulative emissions reductions of 1.4–5.1 Gt require technological innovations within the aluminium sector itself (Supplementary Fig. 3a–c). Enhancing energy efficiency by retrofitting existing smelters and adopting innovative cell designs for new smelters could contribute to 0.5–4.2 Gt cumulative emissions reduction, depending on the electricity source used (P3 versus P4; Fig. 4a and Supplementary Fig. 3a,c).

Implementing inert anode and wettable cathode technologies is crucial to reducing process-related emissions, which currently account for 18% of total GHG emissions from the primary aluminium industry. As electricity sources become more decarbonized, this percentage will increase, making process-related emissions mitigation even more critical. These technologies could achieve 0.8–0.9 Gt in cumulative emissions reduction under different output scenarios (P4 versus P5; Fig. 4a and Supplementary Fig. 3b). This requires retrofitting at least 18% of smelting capacity with inert anode technology by 2040, increasing to 67% by 2050. The high readiness level of inert anode technology in Europe and North America allows for its adoption in these regions before 2035, supported by several pilot projects[40–42]. However, future expansions of primary aluminium production are likely to be concentrated in developing regions such as India, the Middle East and Africa, driven by rapidly growing domestic demand. Given the current lack of a strong foundation for technology R&D in these areas, and with commitments to achieving carbon neutrality extending beyond 2050, new smelting capacity in these developing regions is unlikely to adopt inert anode technology extensively until after 2040 (Fig. 4e–g).

In regions where self-generated electricity is the primary source for aluminium production, China is expected to experience a rapid decrease in emissions across all scenarios, primarily due to the retirement of fossil fuel-based captive power plants and the transition to a cleaner energy generation structure (Fig. 4d). However, other emerging economies face substantial mitigation challenges as their aluminium production grows. Under the BAU scenario (P1), total emissions in India, the Middle East and Africa are projected to increase by 287%, 48% and 314%, respectively, by 2050 compared to 2020 levels (P1, Fig. 4e–g). This highlights the critical need to focus on technological choices for capacity expansion in these emerging economies.

In the short term, key mitigation strategies for aluminium producers in India and the Middle East include halting the construction of new fossil fuel-based captive power plants and planning the retirement of existing ones. In the long term, as electricity generation becomes largely decarbonized, process-related emissions will become the dominant concern, including in Europe and North America (Fig. 4b,c). Therefore, future mitigation efforts in these regions should prioritize technological innovations that address process-related emissions.

https://doi.org/10.1038/s41558-024-02193-x

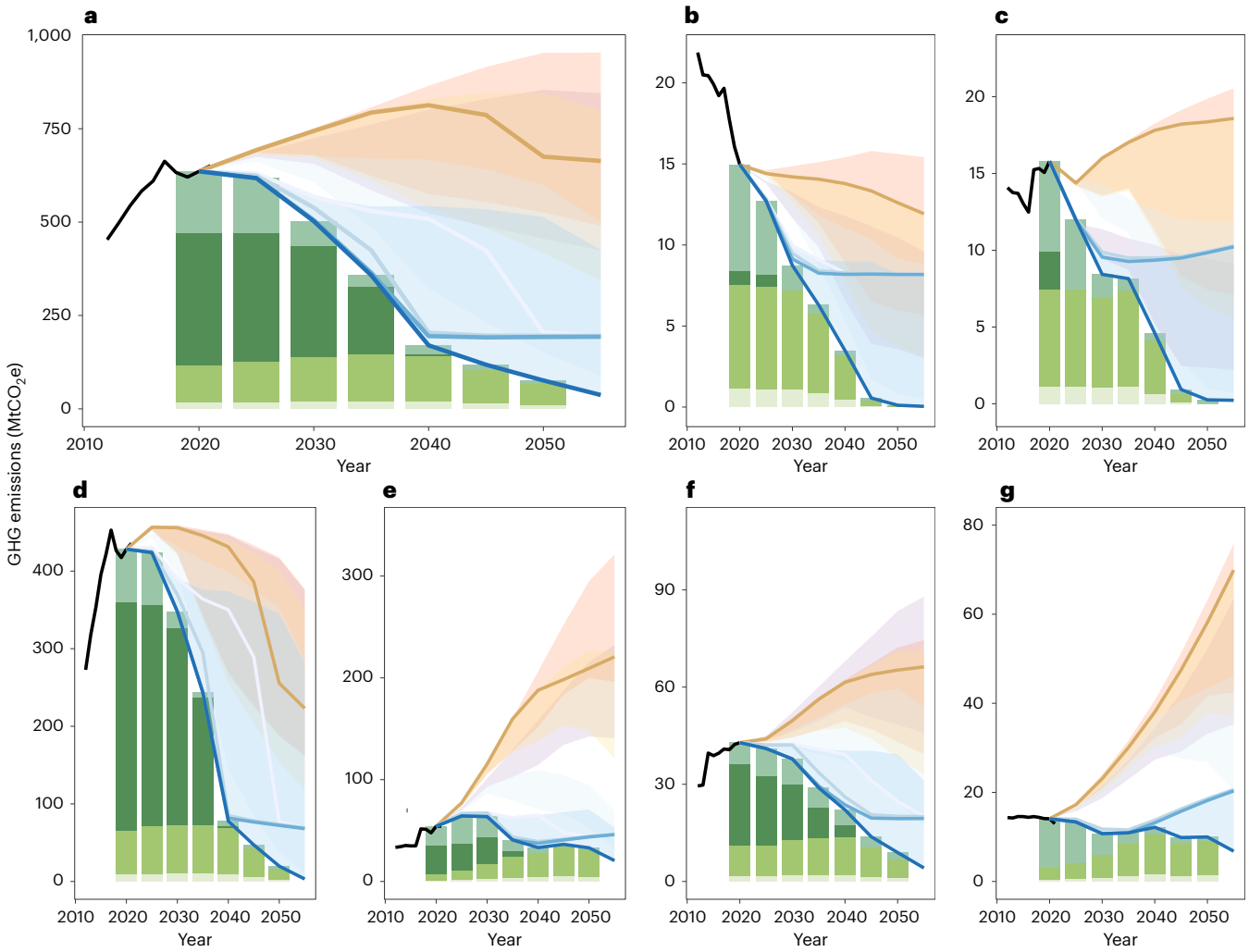

Line colour	Path no.	Path definition	Social-economic driver (SSP)	Captive power plant lifetime (L)	Existing smelter		New smelter
					Commercialized technologies (C)	Inert anode and wettable cathode (E)	Innovative cell design (I)
	P1	Business as usual	SSP245	30 (L_{30})	× (C_1)	× (E_1)	× (I_1)
	P2	P1 + SSP119	SSP119	30 (L_{30})	× (C_1)	× (E_1)	× (I_1)
	P3	P2 + captive early retirement	SSP119	20 (L_{20})	× (C_1)	× (E_1)	× (I_1)
	P4	P3 + energy efficiency improvement	SSP119	20 (L_{20})	✓ (C_2)	× (E_1)	✓ (I_2)
	P5	P4 + process mitigation	SSP119	20 (L_{20})	✓ (C_2)	✓ (E_2)	✓ (I_2)

Fig. 4 | GHG emissions pathways of the aluminium industry. a–g, Total GHG emissions from the primary aluminium smelting sector in global (**a**), Europe (**b**), North America (**c**), China (**d**), India (**e**), Middle East (**f**) and Africa (**g**). The light shaded area represents the range of highest and lowest emissions pathways under the five SSP–RCP scenarios. The bold lines depict the five technology narrative pathways. The bar chart represents the emissions structure under P5, illustrating the most climate-ambitious scenario for the global aluminium industry, which adopts all possible technological strategies to mitigate GHG emissions.

Discussion and conclusion

By developing the CEADs-AGE, we identified the sources of emissions from the global primary aluminium industry from the smelter level upwards. This allowed tailored differentiated mitigation technology packages for global aluminium smelters based on their current cell amperage and electricity sources.

The historical total GHG emissions uncertainty for smelters ranges from 5.3% to 45.3%, with 88% of smelters having uncertainty <20% (Supplementary Fig. 14). This uncertainty may stem from variations in surveyed activity levels, captive power plants and the adopted electricity and process-related emission factors (Supplementary Section 6.1). To improve future accounting accuracy, it is crucial to enhance the spatial and temporal resolution of monitoring smelter electricity structures and the electrolysis process, especially in less developed regions.

Sensitivity analysis indicates that projected cumulative emissions from 2020 to 2050 could vary by −15.5% to +5.6%, depending on the schedule[43] of technology diffusion, energy-saving potential and assumptions about scrap recycling and manufacturing yield[44] (Supplementary Section 7). Regional primary aluminium output levels may be influenced by the patterns of trade in intermediate products,

final goods and recycled scrap. Our study has not yet fully integrated trade and recycling factors into the model, which could introduce fluctuations in regional-level projections. Additionally, new climate pledges, policies, research and pilot projects could alter the pathways of the aluminium sector. Although our study modelled a broad range of SSP–RCP scenarios and diverse technology portfolios, it remains essential to track new trends and continuously incorporate them into future pathway modelling.

Our study focuses solely on GHG emissions from primary aluminium smelting, which accounts for 64–80% of the cradle-to-grave emissions of the entire aluminium production process[45–48]. Other studies have explored strategies such as electrifying or switching to hydrogen-based boilers and calciners to mitigate emissions from alumina refineries[17,49], decarbonizing the casting process[50] and pursuing sustainable bauxite mining practices[51,52]. Future mitigation efforts should encompass the entire supply chain to ensure a systematic approach to decarbonization.

Online content

Any methods, additional references, Nature Portfolio reporting summaries, source data, extended data, supplementary information, acknowledgements, peer review information; details of author contributions and competing interests; and statements of data and code availability are available at https://doi.org/10.1038/s41558-024-02193-x.

References

1. Long, R. S., Boettcher, E. & Crawford, D. Current and future uses of aluminum in the automotive industry. *JOM* **69**, 2635–2639 (2017).
2. Cullen, J. M. & Allwood, J. M. Mapping the global flow of aluminum: from liquid aluminum to end-use goods. *Environ. Sci. Technol.* **47**, 3057–3064 (2013).
3. Wang, S. et al. Future demand for electricity generation materials under different climate mitigation scenarios. *Joule* **7**, 309–332 (2023).
4. Nansai, K. et al. Nexus between economy-wide metal inputs and the deterioration of sustainable development goals. *Resour. Conserv. Recycl.* **149**, 12–19 (2019).
5. Elshkaki, A. & Shen, L. Energy–material nexus: the impacts of national and international energy scenarios on critical metals use in China up to 2050 and their global implications. *Energy* **180**, 903–917 (2019).
6. Moreau, V., Dos Reis, P. C. & Vuille, F. Enough metals? Resource constraints to supply a fully renewable energy system. *Resources* **8**, 29 (2019).
7. Månberger, A. & Stenqvist, B. Global metal flows in the renewable energy transition: exploring the effects of substitutes, technological mix and development. *Energy Policy* **119**, 226–241 (2018).
8. Lennon, A., Lunardi, M., Hallam, B. & Dias, P. R. The aluminium demand risk of terawatt photovoltaics for net zero emissions by 2050. *Nat. Sustain.* **5**, 357–363 (2022).
9. Moreira, S. & Laing, T. *Competitiveness of Global Aluminum Supply Chains Under Carbon Pricing Scenarios for Solar PV* (World Bank, 2023).
10. Hatayama, H., Daigo, I., Matsuno, Y. & Adachi, Y. Evolution of aluminum recycling initiated by the introduction of next-generation vehicles and scrap sorting technology. *Resour. Conserv. Recycl.* **66**, 8–14 (2012).
11. Jones, B., Elliott, R. J. & Nguyen-Tien, V. The EV revolution: the road ahead for critical raw materials demand. *Appl. Energy* **280**, 115072 (2020).
12. Sverdrup, H. U., Ragnarsdottir, K. V. & Koca, D. Aluminium for the future: modelling the global production, market supply, demand, price and long term development of the global reserves. *Resour. Conserv. Recycl.* **103**, 139–154 (2015).
13. Hasanbeigi, A. & Springer, C. How Clean Is the U.S. Steel Industry? *Global Efficiency Intelligence* www.globalefficiency-intel.com/us-steel-industry-benchmarking-energy-co2-intensities (2019).
14. *Primary Aluminium Smelting Power Consumption* (IAI, 2023).
15. Brooks, G. The trouble with aluminium. *The Conversation* http://theconversation.com/the-trouble-with-aluminium-7245 (2012).
16. Making Net-Zero Aluminium Possible. *IAI* https://international-aluminium.org/resource/mpp-and-iai-release-ambitious-decarbonization-aluminium-sector/ (2022).
17. *Making Net-Zero Aluminium Possible: An Industry-Backed, 1.5 °C-Aligned Transition Strategy* (MPP, 2023).
18. Zhao, R., Nowicki, C., Gosselin, L. & Duchesne, C. Energy and exergy inventory in aluminum smelter from a thermal integration point-of-view. *Int. J. Energy Res.* **40**, 1321–1338 (2016).
19. Haraldsson, J. & Johansson, M. T. Review of measures for improved energy efficiency in production-related processes in the aluminium industry—from electrolysis to recycling. *Renew. Sustain. Energy Rev.* **93**, 525–548 (2018).
20. Segatz, M., Hop, J., Reny, P. & Gikling, H. in *Light Metals 2016* (ed. Williams, E.) 301–305 (Springer International, 2016).
21. Dorreen, M. et al. in *Energy Technology 2017* (eds Zhang, L. et al.) 15–25 (Springer International, 2017).
22. Tian, Y., Li, H., Wei, L., Cao, X. & Yin, J. in *Light Metals 2013* (ed. Sadler, B. A.) 567–571 (Springer International, 2016).
23. Feng, N. et al. in *Light Metals 2014* (ed. Grandfield, J.) 517–520 (Springer International, 2016).
24. Yan, F., Dupuis, M., Jianfei, Z. & Shaoyong, R. in *Light Metals 2013* (ed. Sadler, B. A.) 537–542 (Springer International, 2016).
25. Jin, H. *Energy-Saving Technologies and Application for Large-Scale Prebaked Anode Aluminum Reduction Cells* (Northeastern Univ., 2015).
26. Feng, N. et al. in *Essential Readings in Light Metals* Vol. 2 (eds Bearne, G. et al.) 523–526 (Springer International, 2016).
27. Mulder, A. et al. in *Light Metals 2014* (ed. Grandfield, J.) 835–840 (Springer International, 2016).
28. Zhang, W. et al. in *Light Metals 2011* (ed. Lindsay, S. J.) 319–323 (Springer International, 2016).
29. Zeng, S., Li, J., Ren, X. & Zhao, Z. In *Proc. 30th IASTED International Conference on Modelling, Identification and Control* (ed. Hamza, M. H.) 93–98 (ACTA, 2010).
30. Wen, Z., Meng, F. & Chen, M. Estimates of the potential for energy conservation and CO_2 emissions mitigation based on Asian-Pacific Integrated Model (AIM): the case of the iron and steel industry in China. *J. Clean. Prod.* **65**, 120–130 (2014).
31. 2006 IPCC Guidelines for National Greenhouse Gas Inventories. *IPCC* www.ipcc-nggip.iges.or.jp/public/2006gl/ (2006).
32. Yang, S., Zhang, H., Zou, Z., Li, J. & Zhong, X. Reducing PFCs with local anode effect detection and independently controlled feeders in aluminum reduction cells. *JOM* **72**, 229–238 (2020).
33. Coal Power Technologies. *Global Energy Monitor* www.gem.wiki/Coal_power_technologies (2021).
34. Paraskevas, D., Van de Voorde, A., Kellens, K., Dewulf, W. & Duflou, J. R. Current status, future expectations and mitigation potential scenarios for China's primary aluminium industry. *Procedia CIRP* **48**, 295–300 (2016).
35. Pedneault, J., Majeau-Bettez, G., Krey, V. & Margni, M. What future for primary aluminium production in a decarbonizing economy? *Glob. Environ. Change* **69**, 102316 (2021).
36. Liu, G., Bangs, C. E. & Müller, D. B. Stock dynamics and emission pathways of the global aluminium cycle. *Nat. Clim. Change* **3**, 338–342 (2013).
37. He, Y., Zhou, K., Zhang, Y., Xiong, H. & Zhang, L. Recent progress of inert anodes for carbon-free aluminium electrolysis: a review and outlook. *J. Mater. Chem. A* **9**, 25272–25285 (2021).

38. Edenhofer, O., Steckel, J. C., Jakob, M. & Bertram, C. Reports of coal's terminal decline may be exaggerated. *Environ. Res. Lett.* **13**, 024019 (2018).
39. Johnson, N. et al. Stranded on a low-carbon planet: implications of climate policy for the phase-out of coal-based power plants. *Technol. Forecast. Soc. Change* **90**, 89–102 (2015).
40. ELYSIS Selects Alma Smelter for Commercial Size 450 kA Inert Anode Prototype Cells. *ELYSIS* www.elysis.com/en/elysis-selects-alma-smelter-for-commercial-size-450-ka-inert-anode-prototype-cells (2021).
41. Hydro Opens Test Pilot for New Anode Technology. *Hydro* www.hydro.com/en/media/news/2014/hydro-opens-test-pilot-for-new-anode-technology/ (2014).
42. Primary aluminum: inert anode and wettable cathode technology in aluminum electrolysis. *Light Metal Age Magazine* www.light-metalage.com/resources/patents/primary-aluminum-inert-anode-and-wettable-cathode-technology-in-aluminum-electrolysis/ (2020).
43. Yu, X. & Tan, C. China's pathway to carbon neutrality for the iron and steel industry. *Glob. Environ. Change* **76**, 102574 (2022).
44. Langhorst, M., Billy, R. G., Schwotzer, C., Kaiser, F. & Müller, D. B. Inertia of technology stocks: a technology-explicit model for the transition toward a low-carbon global aluminum cycle. *Environ. Sci. Technol.* **58**, 9624–9635 (2024).
45. Paraskevas, D., Kellens, K., Van de Voorde, A., Dewulf, W. & Duflou, J. R. Environmental impact analysis of primary aluminium production at country level. *Procedia CIRP* **40**, 209–213 (2016).
46. Guo, Y., Zhu, W., Yang, Y. & Cheng, H. Carbon reduction potential based on life cycle assessment of China's aluminium industry—a perspective at the province level. *J. Clean. Prod.* **239**, 118004 (2019).
47. *Greenhouse Gas Emissions Intensity—Primary Aluminium* (IAI, 2023).
48. Liu, Z. et al. Uncovering driving forces on greenhouse gas emissions in China's aluminum industry from the perspective of life cycle analysis. *Appl. Energy* **166**, 253–263 (2016).
49. Sáez-Guinoa, J., García-Franco, E., Llera-Sastresa, E. & Romeo, L. M. The effects of energy consumption of alumina production in the environmental impacts using life cycle assessment. *Int. J. Life Cycle Assess.* https://doi.org/10.1007/s11367-023-02257-8 (2023).
50. Liu, W. et al. Scenario analysis on carbon peaking pathways for China's aluminum casting industry. *J. Clean. Prod.* **422**, 138571 (2023).
51. Georgitzikis, K., Mancini, L., Delia, E. & Vidal Legaz, B. *Sustainability Aspects of Bauxite and Aluminium* (Publications Office of the European Union, 2021).
52. Norgate, T. & Haque, N. Energy and greenhouse gas impacts of mining and mineral processing operations. *J. Clean. Prod.* **18**, 266–274 (2010).

Methods

Global aluminium GHG emissions inventory

To construct CEADs-AGE, we began with data from BAIINFO (http://www.baiinfo.com/) based on a smelter survey, which provides monthly data (2018–2021) and yearly data (2012–2017) on smelter capacity, production, amperage configuration, energy intensity and the proportion of self-generated and purchased electricity (the proportion data available only for smelters in China). We then acquired a coal- and gas-based power plant inventory from the Global Energy Monitor (https://globalenergymonitor.org/), which identified 594 captive power units associated with the aluminium industry. By comparing the geographical locations and ownership information of smelters and captive power units, we established the affiliations. After excluding captive power plants linked to alumina refineries and those no longer in operation, we identified 280 operating captive power plant units in 2021.

GHG emissions from primary aluminium production are categorized into four main types: (1) CO_2 emissions from self-generated electricity; (2) CO_2 emissions from grid-purchased electricity; (3) process-related CO_2 emissions; and (4) process-related PFCs (including CF_4 and C_2F_6) emissions. The total emissions of an aluminium smelter are the sum of these four types:

$$E_{s,y} = \mathrm{EE}_{\mathrm{S}_{s,y}} + \mathrm{EE}_{\mathrm{G}_{s,y}} + E_{\mathrm{PC}_{s,y}} + E_{\mathrm{PFC}_{s,y}} \quad (1)$$

Where subscript s and y represents the smelter and year, respectively. E, $\mathrm{EE_S}$, $\mathrm{EE_G}$, E_{PC} and E_{PFC} represent total CO_2 equivalent emissions, self-generated electricity CO_2 emissions, grid-purchased electricity CO_2 emissions, process-related CO_2 emission and PFCs emission (in CO_2e), respectively.

CO_2 emissions from self-generated and grid-purchased electricity are estimated using equations (2) and (3), respectively:

$$\mathrm{EE}_{\mathrm{S}_{s,y}} = \mathrm{AD}_{s,y} \times \mathrm{EI}_{s,y} \times S_{s,y} \times \mathrm{EF}_{\mathrm{S}_{s,y}} \quad (2)$$

$$\mathrm{EE}_{\mathrm{G}_{s,y}} = \mathrm{AD}_{s,y} \times \mathrm{EI}_{s,y} \times (1 - S_{s,y}) \times \mathrm{EF}_{\mathrm{G}_{s,y}} \quad (3)$$

where $\mathrm{AD}_{s,y}$ represents activity data (here referring to production) of smelter s in year y; $\mathrm{EI}_{s,y}$ represents energy intensity of smelter s in year y (in kWh t^{-1} Al); $S_{s,y}$ represents the share of self-generated electricity in the energy supply of smelter s in year y (in %); and $\mathrm{EF}_{\mathrm{S}s,y}$ and $\mathrm{EF}_{\mathrm{G}s,y}$ represent self-generated and grid-purchased electricity emission factor of smelter s at year y, respectively (in $kgCO_2\,kWh^{-1}$).

The activity data, AD, and electricity energy intensity, EI, for smelters are obtained directly from the smelter survey.

For smelters in China, our survey data include the proportion of self-generated electricity. However, for smelters outside China, this information is not available. In these cases, we assume that smelters prioritize using electricity from their captive power plants and only purchase electricity from the local grid if the captive power capacity is insufficient to meet electricity demand. For smelters without captive power plants, we assume that all electricity is sourced from the local grid.

The electricity emission factor of each coal-based captive power plant ($\mathrm{EF}_{\mathrm{S}_{s,y}}$) is obtained from Global Energy Monitor[53]. The electricity emission factor of gas-based power plants is obtained from the literature[54–59]. For the purchased grid electricity emission factor ($\mathrm{EF}_{\mathrm{G}_{s,y}}$), we prioritized data released by government and further collected subnational grid electricity emission factors for Australia[60], Canada[61], China[62] and the United States[63] to replace national-average value since these countries have large territories with several relatively independent power grids; therefore, subnational value could reflect regional variations in electricity supply and emission patterns. For countries where government-released data are unavailable, particularly for less developed countries, we use third-party evaluations, including (1) Carbon Footprint[64]; (2) Climate Transparency[65]; and (3) Low-Carbon Power[66]. Different data sources are cross-compared and either take the average of the three or exclude outliers to calculate the average value for these countries. Supplementary Section 2 describes the details of electricity emission factor collection.

The process-related CO_2 emission from primary aluminium production comes from the consumption of carbon anode during electrolysis:

$$2\mathrm{Al}_2O_3 + 3C \rightarrow 4Al + 3CO_2 \quad (4)$$

We use the IPCC-recommended tier 1 method for process-related CO_2 emission estimation[31]:

$$E_{\mathrm{PC}_{s,y}} = \mathrm{AD}_{s,y} \times \mathrm{EF}_{\mathrm{PC}_{s,y}} \quad (5)$$

where $\mathrm{EF}_{\mathrm{PC}_{s,y}}$ represents emission factor of process-related CO_2.

The process-related PFCs emission comes from the anode effect during smelting. Liquid alumina must be added to the cells periodically to maintain a stable alumina concentration level since alumina is consumed during the electrolysis. Too low/high alumina concentration would result in the gaseous electrical insulation layer around carbon anode and increase of cell voltage, leading to the anode gas composition change from CO_2 to CO and PFCs[31], which is known as the anode effect. We used the IPCC-recommended tier 1 method[31] for process-related PFCs emission estimation as follows:

$$E_{\mathrm{PFC}_{s,y}} = \mathrm{AD}_{s,y} \times \mathrm{EF}_{\mathrm{PFC}_{s,y}} \quad (6)$$

where $\mathrm{EF}_{\mathrm{PFC}_{s,y}}$ represents emission factor of process-related PFCs (in $tCO_2e\ t^{-1}$ Al).

The process-related CO_2 emission factors are from International Aluminium Institute (IAI)[47]. The PFCs emission factors for smelters in China are from our previous study[67], which adjusts the emission factor according to technology structure in China. The PFCs emission factors for smelters beyond China are from IAI[47]. Supplementary Table 2 lists all the adopted process-related emission factors.

Emissions projection of global aluminium smelters

Similar to GHG emissions accounting framework stated above, the future emissions projection of each smelter is also based on seven parameters under three categories: mitigation technology (includes energy intensity, process-related PFCs and CO_2 emission factors), electricity source (includes share of self-generated electricity, emission factor for self-generated and grid-purchased electricity) and smelter production (Extended Data Fig. 2). Here we set a series of subscenario combinations to explore the possible future trajectory of each smelter.

We examined five socioeconomic development subscenarios by combining various shared SSPs and RCPs to provide a detailed picture of potential futures by linking socioeconomic development with climate forcing. This impacts aluminium production projections and electricity generation pathways, thereby influencing the GHG emissions trajectory of primary aluminium production. The five typical SSP–RCP combinations are:

- SSP360: SSP3–RCP6.0. High population growth but low GDP growth. Relatively high fossil fuel-based with slow progress in renewables.
- SSP260: SSP2–RCP6.0. Moderate GDP and population growth. Relatively high fossil fuel-based with slow progress in renewables.
- SSP245: SSP2–RCP4.5. Moderate GDP and population growth. A balanced energy mix with gradual growth in renewables.
- SSP126: SSP1–RCP2.6. High GDP growth, low population growth. Rapid transition to renewables, substantial reduction in fossil fuel.

- SSP119: SSP1–RCP1.9. High GDP growth, low population growth. Near-total renewable energy dominance, aggressive decarbonization.

The five SSP–RCP combination pathways are simulated using GCAM v.6.0, a widely used integrated assessment model[68–71]. GCAM v.6.0, released in 2022, divides the world into 32 regions, uses 2015 as the base year and projects the future in 5 year time steps[72]. Besides the five SSP–RCP subscenarios (SSP), we also introduce four technology application subscenario sets, including:

- Three scenarios considering different lifetimes of captive power plants (L).
- Two commercialized technology subscenarios (C).
- Two inert anode and wettable cathode technology subscenarios (E).
- Two innovative cells design subscenarios (I).

Each subscenario set is used to determine one or several parameters. Extended Data Fig. 2 summarizes how each subscenario impacts the parameters and thus the GHG emissions from the aluminium smelter. We treat each scenario as the different combinations of the individual subscenarios (SSP, L, C, E, I) such that we will have $5 \times 3 \times 2 \times 2 \times 2 = 120$ possible scenarios.

Scenario settings

Socioeconomic pathway. The GHG emissions of each smelter are influenced by three macro-socioeconomic factors: (1) electricity cost, (2) energy mix of electricity generation and (3) primary aluminium production (Extended Data Fig. 3) as outlined below.

Decision on new captive power plants. The decision to equip newly built smelting capacity with captive power plants is based on a cost comparison between fossil fuel power generation (mainly coal and gas) and grid-purchased electricity. Smelters typically opt for the cheaper electricity source. Detailed modelled electricity costs are provided in Supplementary Figs. 8–12.

Grid-purchased electricity emission factors. For smelters without captive power plants, the emission factor for grid-purchased electricity depends on the regional electricity generation mix. We assume that the grid electricity emission factor follows the same trend for all smelters within the same region. As a result, we apply the regional electricity emission factor trend to each smelter in the corresponding region. The modelled trend is shown in Supplementary Fig. 7.

Smelter-level output. Smelters adjust their production to meet the demand for regional primary aluminium production. If the current operating capacity is insufficient to meet this demand, new capacity must be built. Achieving a 100% capacity factor is challenging as a result of maintenance, energy supply fluctuations and operational inefficiencies, leading to actual operating capacity being lower than installed capacity. Therefore, the new-built smelting capacity of region r in year y is calculated as follows:

$$\begin{aligned}\text{New\_Capacity}_{r,y} &= 0\ (\text{if}:\ \text{Capacity}_{r,y-1}U_f \geq \text{Output}_{r,y})\\ \text{New\_Capacity}_{r,y} &= (\text{Output}_{r,y} - \text{Capacity}_{r,y-1}U_f)/U_f\\ &\quad (\text{if}:\ \text{Capacity}_{r,y-1}U_f < \text{Output}_{r,y})\end{aligned} \tag{7}$$

Where U_f represents maximum utilization factor of smelters. Currently, global average utilization factor is 85%; we assume this capacity utilization factor will keep in the projection. Total aluminium smelting capacity of region r in year y can be obtained as:

$$\text{Capacity}_{r,y} = \text{Capacity}_{r,y-1} + \text{New\_Capacity}_{r,y} \tag{8}$$

We allocate the regional primary aluminium output to each smelter according to both its efficiency and capacity. If the regional output reaches the maximum operating capacity, then each smelter should operate at its maximum utilization factor. Otherwise, the smelters in the region are ranked from lowest to highest in terms of energy intensity, and this ranking is used to prioritize production to the most efficient smelters. AO represents the ascending order. The order of smelters in terms of energy intensity from lowest to highest is as follows:

$$\mathbf{s} = \text{AO}(\text{EI}_{s,y}) \tag{9}$$

The aluminium output of the nth ranked smelter in region r and year y can be written as:

$$\begin{aligned}\text{AD}_{n,y} &= \text{Capacity}_{n,y}U_f\ (\text{if}:\ \text{Output}_{r,y} \geq \sum_{s=1}^{n}\text{Capacity}_{s,r,y}U_f)\\ \text{AD}_{n,y} &= \text{Output}_{r,y} - \sum_{s=1}^{n-1}\text{AD}_{s,r,y}\ \Bigg(\text{if}:\ \text{Output}_{r,y} > \sum_{s=1}^{n-1}\text{Capacity}_{s,r,y}U_f \wedge\\ &\qquad \text{Output}_{r,y} < \sum_{s=1}^{n}\text{Capacity}_{s,r,y}U_f\Bigg)\\ \text{AD}_{n,y} &= 0\ (\text{if}:\ \text{Output}_{r,y} < \sum_{s=1}^{n-1}\text{Capacity}_{s,r,y}U_f)\end{aligned} \tag{10}$$

The future aluminium output growth is driven by GDP, income elasticities and price elasticities in GCAM:

$$\text{Output}_{r,t} = \text{Output}_{r,t-1}\left(\frac{Y_{r,t}}{Y_{r,t-1}}\right)^{\alpha}\left(\frac{P_{r,t}}{P_{r,t-1}}\right)^{\beta}\left(\frac{N_{r,t}}{N_{r,t-1}}\right) \tag{11}$$

where Y is the per capita GDP, P is the price of industry service (here, mainly primary aluminium price), N is the population and α and β are income and price elasticities, respectively.

The modelled regional primary production output can be found in Supplementary Fig. 6. Supplementary Fig. 23 gives the comparison of primary aluminium production projection with existing literature.

Captive power plant lifetime. The lifetimes of captive power plants determine when an existing unit will cease operation, thereby affecting the share of self-generated electricity. Previous studies indicate that the typical lifetime of thermal generation units ranges from 30 to 50 years[38,39], with the widest reported range being 20–60 years[73]. To evaluate the impact of shorter or longer operational periods of captive power plants on the GHG emissions of the aluminium sector, we define three subscenarios:

- L_{40}: lifetime = 40 years.
- L_{30}: lifetime = 30 years.
- L_{20}: lifetime = 20 years.

Commercialized technology. The implementation of commercialized energy-saving technologies will influence the energy intensity of each smelter. Figure 2 illustrates the range of energy-saving potential for each technology, while Supplementary Section 3 provides a detailed description. We define two subscenarios for commercialized technologies:

- C_1: without the application of commercialized technologies.
- C_2: with the application of commercialized energy-saving technologies for retrofitting existing smelters. The technology diffusion follows an S-shaped logistic curve (Supplementary Section 4) and we apply the average energy-saving potential of each technology.

Inert anode and wettable cathode. The adoption of inert anode and wettable cathode technology will result in process-related CO_2 and PFCs emissions being reduced to zero (Supplementary Sections 3.14 and 3.15). We define two subscenarios for the application of this technology:

- E_1: without the application of inert anode and wettable cathode technology
- E_2: with the application of inert anode and wettable cathode technology to all smelters, once the necessary technology readiness level is reached

Here, E represents the retrofitting of electrodes (anode and cathode). The timing for when a smelter can be retrofitted with inert anode and wettable cathode technology depends on the technology readiness level of the parent company and the climate ambition of the region. The diffusion rate of the technology follows an S-shaped logistic curve (Supplementary Section 4).

Innovative cell design. The application of innovative cell design will affect the energy intensity of newly built smelting capacity (Supplementary Section 3). We define two subscenarios for the adoption of innovative cell design:

- I_1: without the application of innovative cell design
- I_2: with innovative cell design applied to new smelting capacity once the technology reaches the necessary readiness level

Description of selected technology narrative pathways

Pathway P1 (SSP245, L_{30}, C_1, E_1, I_1) is a BAU scenario. Global primary aluminium production levels and regional electricity generation pathways are based on the SSP245 scenario, which is widely used as a baseline in research[74–76] and aligns with current global development trends[77–79]. No additional mitigation technologies are adopted within the aluminium sector and the lifetime of captive power plants follows the default value of 30 years.

Pathway P2 (SSP119, L_{30}, C_1, E_1, I_1) is based on P1 but shifts the aluminium production projection and regional electricity pathways to SSP119. It represents a scenario where the aluminium sector does not undertake any additional mitigation efforts, with emissions decreasing as a result of the decarbonization of grid power.

Pathway P3 (SSP119, L_{20}, C_1, E_1, I_1) builds on P2; this pathway shortens the lifespan of captive power plants from 30 to 20 years.

Pathways P4 and P5 each build on the previous one by incorporating additional mitigation strategies. Specifically, they adopt commercialized technologies and innovative cell design to improve smelter energy efficiency, as well as inert anode and wettable cathode technologies to mitigate process-related emissions. Pathway P5 (SSP119, L_{20}, C_2, E_2, I_2) represents the most aggressive mitigation scenario, where the aluminium sector adopts all possible strategies, including both current and future technologies, early retirement of captive power plants and a high penetration of renewable energy in the regional electricity generation mix, as outlined in SSP119.

Data availability

Data can be accessed through https://www.ceads.net/user/downspecial.php?id=1428.

Code availability

The code of GCAM v.6.0 model is open-source and can be obtained from https://jgcri.github.io/gcam-doc/v6.0/overview.html.

References

53. *Power Plants* (Global Energy Monitor, 2022)
54. Sieker, T. et al. Emission footprint analysis of dispatchable gas-based power generation technologies. *Vgbe Energy J.* **7**, 32–43 (2022).
55. Liu, H., Zhou, S., Peng, T. & Ou, X. Life cycle energy consumption and greenhouse gas emissions analysis of natural gas-based distributed generation projects in China. *Energies* **10**, 1515 (2017).
56. *Emissions by Plant and by Region* (EIA, 2023).
57. Emission Factor: Electricity Supplied from Natural Gas CCGT Power Plant. *Climatiq* www.climatiq.io/data/emission-factor/7bfab478-b1e7-4ded-9907-9f200b40f2cb (2024).
58. Nicholson, S. & Heath, G. *Life Cycle Emissions Factors for Electricity Generation Technologies* (NREL, 2021).
59. *Survey of Combined Cycle Combustion Turbine Greenhouse Gas Emission Rates* (State of Washington, 2012); https://app.leg.wa.gov/ReportsToTheLegislature/Home/GetPDF?fileName=Survey%20of%20Commercially%20Available%20Turbines_FINAL_11%205%2012%20pdf_a776d3a6-d603-42ad-b998-19bbf1c98a31.pdf
60. *National Greenhouse Accounts Factors* (DCCEEW, 2024); https://www.dcceew.gov.au/climate-change/publications?k=National+Greenhouse+Accounts+Factors
61. The Environment and Climate Change Canada Data Catalogue. *Government of Canada* https://data-donnees.az.ec.gc.ca/data/substances/monitor/?lang=en (2024).
62. Cai, B. et al. *China Regional Power Grids Carbon Dioxide Emission Factors* (CAEP, 2023); www.caep.org.cn/sy/tdftzhyjzx/zxdt/202310/W020231027692141725225.pdf
63. Emissions & Generation Resource Integrated Database (eGRID). *EPA* www.epa.gov/egrid (2024).
64. International Electricity Factors. *Carbon Footprint* www.carbonfootprint.com/international_electricity_factors.html (2023).
65. Climate Transparency Report 2022. *Climate Transparency* www.climate-transparency.org/g20-climate-performance/g20report2022 (2024).
66. Low-Carbon Power: Monitor the Transition to Low Carbon Energy. *Low-Carbon Power* https://lowcarbonpower.org/ (2022).
67. Yu, X. & Tan, C. China's process-related greenhouse gas emission dataset 1990–2020. *Sci. Data* **10**, 55 (2023).
68. Calvin, K. et al. GCAM v5.1: representing the linkages between energy, water, land, climate, and economic systems. *Geosci. Model. Dev.* **12**, 677–698 (2019).
69. Tong, D. et al. Dynamic projection of anthropogenic emissions in China: methodology and 2015–2050 emission pathways under a range of socio-economic, climate policy, and pollution control scenarios. *Atmos. Chem. Phys.* **20**, 5729–5757 (2020).
70. Calderón, S. et al. Achieving CO_2 reductions in Colombia: effects of carbon taxes and abatement targets. *Energy Econ.* **56**, 575–586 (2016).
71. Shi, W. et al. Projecting state-level air pollutant emissions using an integrated assessment model: GCAM-USA. *Appl. Energy* **208**, 511–521 (2017).
72. GCAM v6 Documentation: GCAM Model Overview. *JGCRI* http://jgcri.github.io/gcam-doc/overview.html (2022).
73. Davis, S. J. & Socolow, R. H. Commitment accounting of CO_2 emissions. *Environ. Res. Lett.* **9**, 084018 (2014).
74. Niu, J. et al. Projection of future carbon benefits by photovoltaic power potential in China using CMIP6 statistical downscaling data. *Environ. Res. Lett.* **18**, 094013 (2023).
75. Li, S.-Y. et al. Projected drought conditions in Northwest China with CMIP6 models under combined SSPs and RCPs for 2015–2099. *Adv. Clim. Chang. Res.* **11**, 210–217 (2020).
76. Su, B. et al. Insight from CMIP6 SSP–RCP scenarios for future drought characteristics in China. *Atmos. Res.* **250**, 105375 (2021).
77. NDC Synthesis Report. *UNFCCC* https://unfccc.int/process-and-meetings/the-paris-agreement/nationally-determined-contributions-ndcs/ndc-synthesis-report/ndc-synthesis-report#Projected-GHG-emission-levels (2021).

78. NDC Synthesis Report. *UNFCCC* https://unfccc.int/ndc-synthesis-report-2022 (2022).
79. NDC Synthesis Report. *UNFCCC* https://unfccc.int/ndc-synthesis-report-2023 (2023).

Acknowledgements

We thank the Carbon Neutrality and Energy System Transformation programme and are grateful for comments by reviewers. This research is funded by the National Key R&D Program of China (2022YFE0208500), the National Natural Science Foundation of China (72473153), International Joint Mission on Climate Change and Carbon Neutrality, the Beijing Natural Science Foundation (International Scientists Project: IS23124) and the Research Grants Council of the Hong Kong Special Administrative Region, China (AoE/P-601/23-N).

Author contributions

Conceptualization: C.T., X.Y., D.G., T.L. Methodology: C.T., X.Y., D.G., T.L. Investigation: C.T., D.L., Q.H. Visualization: C.T. Funding acquisition: X.Y., D.G. Writing—original draft: C.T. Writing—review and editing: C.T., X.Y., D.G.

Competing interests

The authors declare no competing interests.

Additional information

Extended data is available for this paper at https://doi.org/10.1038/s41558-024-02193-x.

Supplementary information The online version contains supplementary material available at https://doi.org/10.1038/s41558-024-02193-x.

Correspondence and requests for materials should be addressed to Xiang Yu or Dabo Guan.

Peer review information *Nature Climate Change* thanks Julien Pedneault, Sven Teske and the other, anonymous, reviewer(s) for their contribution to the peer review of this work.

https://doi.org/10.1038/s41558-024-02193-x

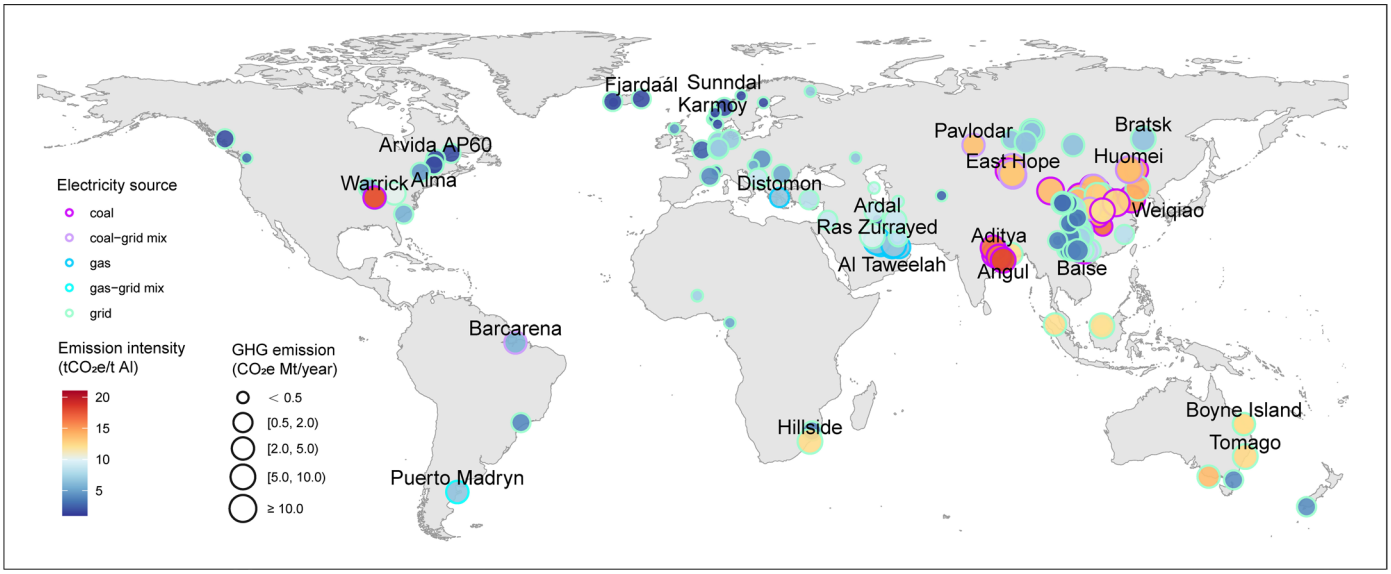

Extended Data Fig. 1 | Map of GHG emissions of aluminum smelters in 2021. The emissions intensity (in tCO2e/t Al) of smelters are represented by the dot inner color. The outer color of the dots indicates the composition of smelter's electricity sources, including coal- or gas-based captive power plants, purchased electricity from the grid, and a mixture of the two. Smelter's total GHG emissions (in Mt CO2e) are represented by the size of the dot.

https://doi.org/10.1038/s41558-024-02193-x

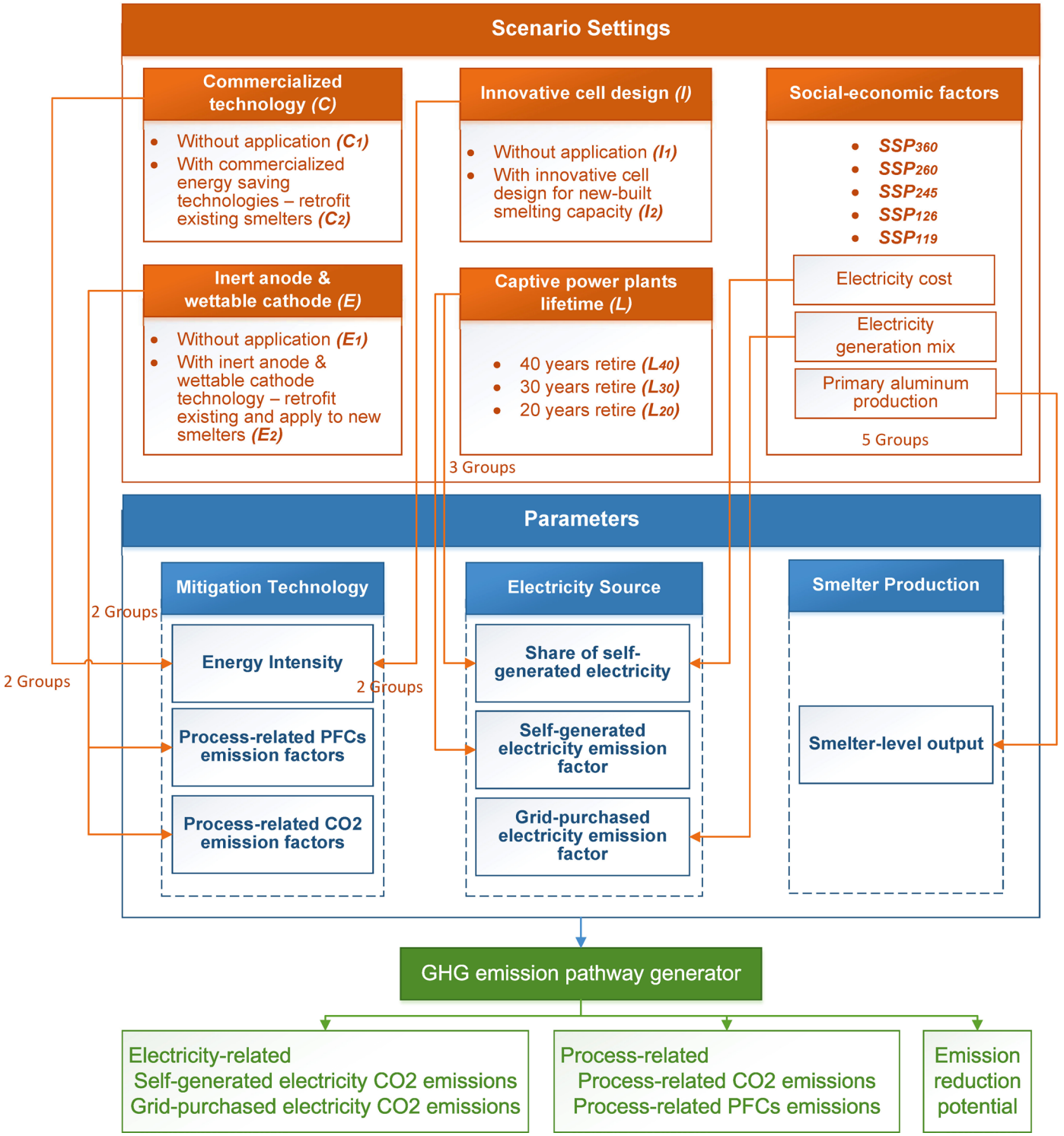

Extended Data Fig. 2 | Aluminum smelter GHG emissions projection framework. The blue part illustrates the parameters that impact the GHG emissions pathways. The orange part illustrates the sub-scenario sets, with each of the sub-scenario determining one or several parameters. Sub-scenario sets are combined to generate combined emissions pathways for global primary smelters as well as the emission reduction potential, which are illustrated in green.

https://doi.org/10.1038/s41558-024-02193-x

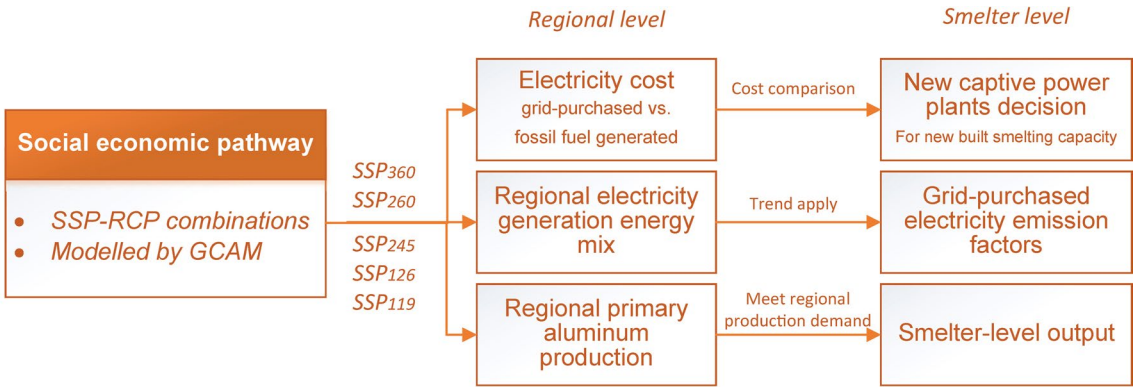

Extended Data Fig. 3 | SSP-RCPs link with aluminum smelter in emission projection. Five SSP-RCP scenarios are modeled using GCAM. Regional electricity costs, electricity generation energy mix, and projections for primary aluminum production are extracted from these scenarios. These factors will then influence decisions on new captive power plants, the emission factor of grid-purchased electricity, and the smelter-level output of each facility.

https://doi.org/10.1038/s41558-024-02193-x

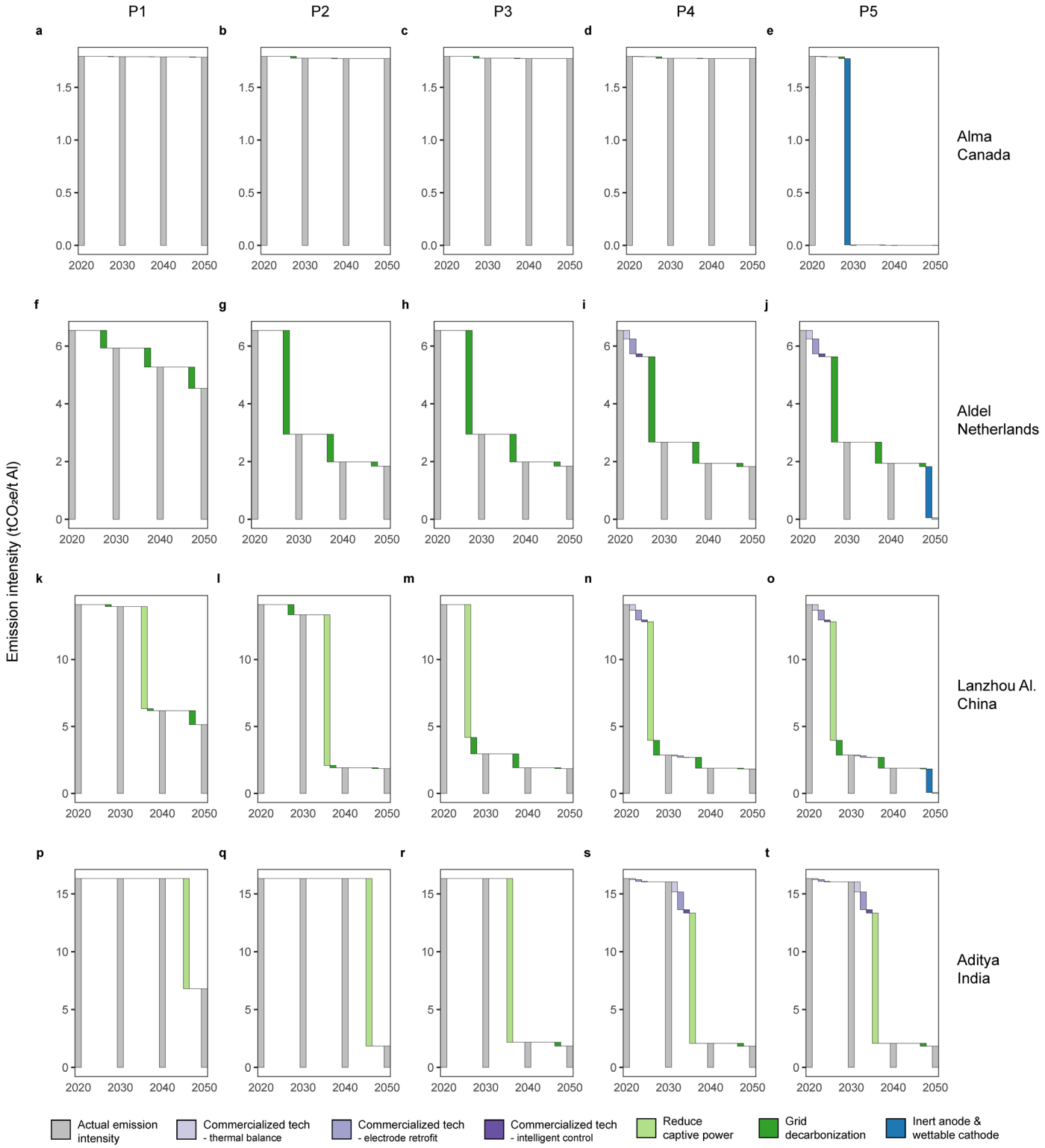

Extended Data Fig. 4 | Technology emission reduction contributions. The contribution of different technologies to reducing the emissions intensity. Each row represents the emissions intensity trend of a typical aluminum smelter under five technology narrative pathways (P1 - P5). **a**–**t**, Alma, Canada (**a**–**e**); Aldel, Netherlands (**f**–**j**); Lanzhou Al., China (**k**–**o**); and Aditya, India (**p**–**t**). See Table 1 for the definitions of narrative pathways. The four typical smelters shown here are the same as those depicted in Fig. 3 of the manuscript.